Available online at www.sciencedirect.com
ScienceDirect
C. R. Physique 9 (2008) 850–856
COMPTES RENDUS PHYSIQUE
http://france.elsevier.com/direct/COMREN/

Recent advances in quantum dot physics / Nouveaux développements dans la physique des boîtes quantiques

Cavity QED effects with single quantum dots

Antonio Badolato [a,*], Martin Winger [a], Kevin J. Hennessy [b], Evelyn L. Hu [b], Ataç Imamoğlu [a]

[a] *Institute of Quantum Electronics, ETH Zurich, 8093 Zurich, Switzerland*
[b] *California NanoSystems Institute, University of California, Santa Barbara, CA 93106, USA*

Available online 18 November 2008

Abstract

A single quantum dot embedded in a photonic crystal defect cavity allows for the investigation of cavity quantum electrodynamics effects in a solid-state environment. We present experiments demonstrating the quantum nature of this fundamental system in the strong coupling regime. Photon correlation measurements are used to characterize the fundamental properties of this unique system: through these experiments, we identify an unexpected, efficient sustaining mechanism that ensures strong cavity emission and is quantum correlated with the exciton resonance, even when all the quantum dot resonances are far detuned from the cavity mode. ***To cite this article: A. Badolato et al., C. R. Physique 9 (2008).***

Résumé

Effets d'électrodynamique quantique de cavité avec des boîtes quantiques uniques. Une boîte quantique unique insérée dans la cavité induite par un défaut d'un cristal photonique permet d'étudier les effets d'électrodynamique quantique de cavité en milieu solide. Nous présentons des expériences démontrant la nature quantique de ce système dans le régime de couplage fort. Des mesures de corrélation de photons permettent de caractériser les propriétés fondamentales de ce système original : grâce à ces expériences, nous identifions un mécanisme sous-jacent inattendu et efficace qui assure une émission de cavité intense et est corrélé de manière quantique à la résonnance excitonique, même quand toutes les résonnances de la boîte quantique sont loin de l'accord avec le mode de cavité. ***Pour citer cet article : A. Badolato et al., C. R. Physique 9 (2008).***

Keywords: Semiconductor; Quantum dot; Photonic crystal; Cavity quantum electrodynamics; Quantum optics; Vacuum Rabi splitting; Quantum information

Mots-clés : Semi-conducteur ; Cristal photonique ; Électrodynamique quantique de cavité ; Optiques quantiques ; Information quantique

1. Introduction

Single atoms, coupled to single cavity radiation field modes, constitute the basic system in cavity quantum electrodynamics (CQED) [1]. Landmark experiments on atoms in cavities have revealed fundamental aspects of quantum

* Corresponding author.
E-mail address: badolato@phys.ethz.ch (A. Badolato).

1631-0705/$ – see front matter
doi:10.1016/j.crhy.2008.10.015

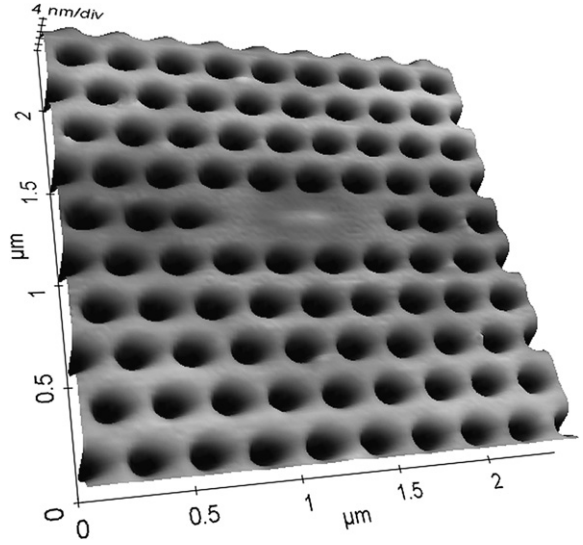

Fig. 1. AFM topography of the L3 type PCM. The first order mode, which is located at the center of the line defect of three missing air holes, is aligned to a small detectable bump tracing one embedded InAs/GaAs QD.

physics, such as continuous collapse of the cavity wave-function upon photon number measurement and decoherence of Schrödinger-cat-like states of light [1]. Recent progress in crystal growth and nanofabrication have made possible the realization of analogous CQED systems in the solid state [2–4]. In particular, semiconductor InAs/GaAs self-assembled quantum dots (QDs) grown by molecular beam epitaxy [5–7] allow for monolithic integration in high-finesse microcavities and exhibit key atom-like features, such as: (i) photon antibunching of the exciton emission [8]; (ii) absorption and emission exciton linewidths approaching the radiative broadening limit [9–11]; and (iii) vacuum Rabi splitting when coupled to high-finesse microcavities [12–17]. Solid state optical cavities typically confine photons by modulation of the refractive index. In photonic crystal structures, Bragg-scattering determined by the periodic dielectric structures prevents light from propagating at certain frequencies (photonic band gap) [18]. Dielectric defects introduced in such a regular structure (Fig. 1) can determine regions where photons remain confined in sub-wavelength mode volumes [19,20].

In this article, we review some of our recent contributions to solid state CQED. In Section 2, we will show how the CQED strong coupling regime can be observed in a truly deterministic fashion by coupling photonic crystals slab microcavities (PCMs) to QDs [12,21]. In Section 3, we will review the off-resonance emission of the PCM and the remarkable antibunching signatures in exciton-cavity photon cross-correlation measurements.

2. Solid state CQED in the strong coupling regime

In a cavity mediated atom-field interaction, the coherent coupling rate between atom and single cavity mode, g_0, competes against two main incoherent decay rates: γ, the rate with which an excited atom can spontaneously emit light out of the cavity mode or recombine non-radiatively, and κ, the decay rate of the cavity field. Because g_0 is highest when the atom is located at the maximum of the cavity mode electric field, it is important to have the atom at that position. Coupling a cavity mode with an atomic transition needs also control of the spectral matching, and optimally with continuous tuning. Achieving an ideal spatial and spectral matching in systems where artificial-atoms are monolithically integrated with microcavities has been one of the most challenging tasks to master for solid state CQED.

2.1. Spatial and spectral matching

QDs nucleate randomly in the growth plane and with a typical inhomogeneous broadening of the interband transitions of ≈ 50 meV. To ensure that some QDs spatially and spectrally match the cavity mode, a common and successful practice has been the fabrication of many microcavities in a high QD density region [13–17,22]. It is clear, however,

that to validate the full potential of the solid state implementation of CQED, a deterministic approach to the spatial and spectral match is needed. Significant progresses towards this direction have been reached both building on nucleation-site-controlled QDs [23–25] and on precise positioning of single microcavity modes around preselected QDs [21,26].

In Fig. 1 we present a demonstration of the latter approach with a L3 type PCM [27,28] fabricated in the low QD density region ($\approx 10^6$ cm^{-2}). The PCM first order mode (which is at the center of the line defect of three missing air holes) was accurately aligned around a small bump tracing a single embedded QD [12,21]. The semiconductor heterostructure was grown on a (100) intrinsic GaAs substrate and formed by a GaAs buffer layer, an $Al_{0.7}Ga_{0.3}As$ sacrificial layer of 1 μm followed by 126 nm of GaAs membrane incorporating in the center a single layer of InAs QDs with a density gradient. To blue-shift the QD emission ($\lambda < 1$ μm) we used the partly covered island technique [7]. The relative position of the bump with respect to metallic markers was determined by atomic force microscopy (AFM) metrology. We emphasize that a crucial advantage of this technique is the pre-selection of QDs with desirable spectral properties. These properties remain unaffected by the hole–air–surfaces created by the fabrication, since the electric field intensity of the L3 first order mode is maximum at the center of the PCM defect [29]. Benefiting from this control over the spatial match, which optimizes the coherent coupling, we were able to achieve vacuum Rabi splitting ($2g_0$) in excess of 300 μeV [30].

To achieve spectral matching of the QD-microcavity system, monolithic microcavities can be initially designed to target a certain spectral range, by adjusting the relevant lithographic parameters; for PCMs those would be the lattice constant a and the hole radius r of the bulk photonic crystal [31]. While relative tuning between devices with different lithographic specifications can be predictable, the precise mode wavelength is highly sensitive to very small deviations close to the mode region. Thus a post-fabrication tuning technique is necessary to tune the cavity mode on resonance with the desired QD transition. Spectral tuning at cryogenic temperature (similar to 4.2 K) has been achieved both by shifting the QD emission and by shifting the microcavity mode emission after fabrication.

The QD emission can be red-shifted relative to the mode emission by increasing the temperature. This approach, however, allows for a maximum wavelength tuning of $\Delta\lambda \approx 1$ nm before the incoherent coupling to the phonon reservoir becomes significant. A more versatile approach is the post-fabrication tuning of microcavities like microdisks [32,33] and PCMs, which allow for a wide manipulation due to the accessibility of the mode by external means. Micropillars, which demonstrate impressive out-coupling efficiency [34–36], have shown a lower post-fabrication tunability [37]. PCM tuning techniques include digital etching [21,38], discriminate mode tuning by AFM nano-oxidation [39], tuning by near-field probes [40–42], and gas physisorption on the surface of the microcavity [43,44]. The latter technique is particularly useful because it allows for reversible and continual red-shift of the PCM mode over $\Delta\lambda \approx 8$ nm range (depending on the cavity design and cryostat geometry) without detriment of the quality factor (Q). In combination with the aforementioned spatial matching this continual tuning allowed us to probe the fine structure of a single QD strongly coupled to a PCM [30].

L3 type PCMs are particularly suitable for implementing CQED because of the ultra-low effective mode volume, $0.7(\lambda/n)^3$, and a theoretical Q-value of 3×10^5. However, actual GaAs based PCMs in the spectral range $\lambda \approx 1.1$ μm show Q-values that are lower by one order of magnitude ($\approx 3 \times 10^4$). This extra loss does not seem to be caused by photonic crystal disorder. The striking dependence of the PCM losses on the wavelength range and material composition (also reported for microdisk resonators [45]) is primarily attributed to absorption by surface-states in the holes strictly close to the PCM mode.

2.2. The strong coupling regime

In the strong coupling regime the coherent interaction between the QD and the cavity mode prevails over any dissipation in the system (i.e. $g_0 > \max[\gamma, \kappa]$), and the excited atomic state undergoes damped Rabi oscillations at angular frequency g_0. In the emission spectrum, this leads to the splitting of the bare atomic and cavity resonances in two symmetric peaks (blue and red dressed state) with linewidth of $(\gamma + \kappa)/2$ and split by $2g_0$ [46]. Because the anharmonic atom-like behavior in semiconductors is the result of a many-body interaction, it is important to understand whether and when the cavity-coupled-material behaves like a single two-level atom. To a good extent, an InAs/GaAs QD acts as a single two-level system, and therefore the QD-exciton–photon strong coupling can be modeled as a Jaynes–Cummings system. In contrast, other materials like semiconductor quantum well (QW) excitons in the linear regime (i.e. when exciton–exciton interaction can be neglected) behave like harmonic oscillators (i.e. bosons) [47,48],

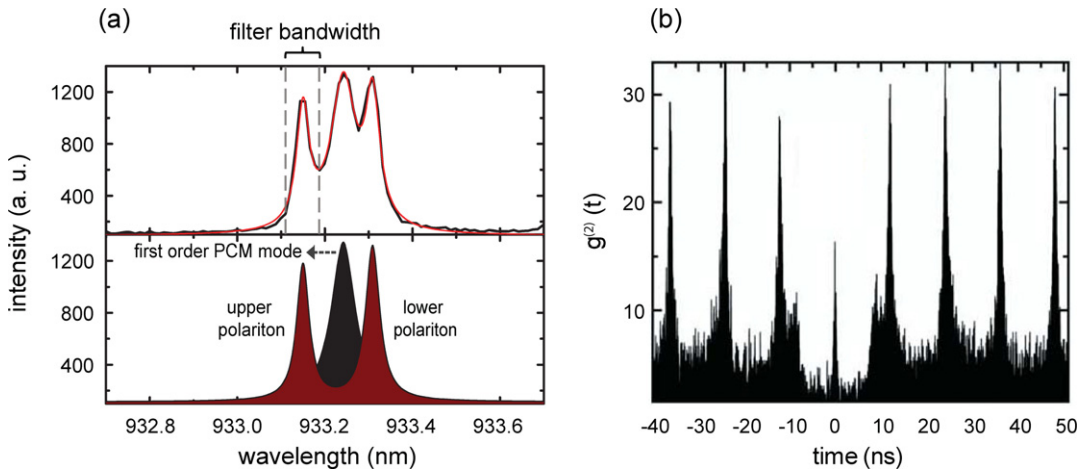

Fig. 2. (a) The upper plot shows the photoluminescence emission spectrum (black line) of a strongly coupled QD-PCM system ($Q = 16\,000$ and $g_0 = 110$ μeV) with ≈ 0.15 nm detuning. The red line in the upper plot and the lower plot show a three-Lorentzian fit. (b) Photon auto-correlation carried out on the upper polariton, which was spectrally filtered with the indicated bandwidth to minimize the contribution of the bare cavity emission (black Lorentzian). The peak at $\tau = 0$ shows 19% in area of peaks at other times. (The two shoulders at $\approx \pm 10$ ns arise from secondary emission from the avalanche photodiodes.)

and QW-exciton–photon in the strong coupling regime shows the normal mode splitting of two strongly coupled linear harmonic oscillators. The two systems, QW-exciton–photon and QD-exciton–photon, behave identically when they exchange one quantum of energy (low excitation regime); the observation of Rabi splitting does not discern between the two cases. With two quanta of energy, however, the QW-exciton–photon system remains harmonic while the QD-exciton–photon system features a non-linearity at single quantum level. Experimental direct evidence of this quantum non-linear regime was observed in microwave cavity QED with atoms [49,50] and superconducting circuits [51], and at optical frequencies with atoms [52]. The anharmonicity was also inferred by observing that a Poissonian stream of photons incident on a strongly coupled atom-cavity system was converted into a sub-Poissonian, anti-bunched stream [53].

In Fig. 2(a) we show the spectrum of a strongly coupled QD-PCM system. The deterministic spatial and spectral match on this device yielded coupling strength $g_0 = 110$ μeV. As we discussed in Ref. [12], the center peak (black colored) is the bare cavity emission, which appears when the QD emission switches to a different frequency due to Stark fields induced by charge fluctuation in the QD proximity. In resonant scattering experiments performed in reflection scheme on the same device, we observed the same g_0 value while the center peak quenched at pump powers below ≈ 10 pW. This indicates that when there is only one QD coupled to the PCM mode the system is extremely sensitive to charge fluctuations triggered by the incident laser.

The large splitting and the small detuning (Fig. 2(a)) allowed us to filter the emission of the blue dressed state (upper polariton) and measure two-photon correlation in a Hanbury Brown–Twiss set-up. Under pulsed excitation (pumping above the GaAs band-gap), we measured sub-Poissonian light (Fig. 2(b)) emitted by the upper polariton: this observation gives an indirect signature of the quantum non-linearity of the QD-PCM system.

3. Off-resonance cavity emission

One of the most striking difference between CQED with atoms and CQED with QDs has been the observation of cavity-mode emission off-resonance. This has now been reported by many groups regardless of the microcavity structure being used [17,54,55]. The phenomenology that we observed in off resonance PCM-QD systems is common to all our devices [56]: (i) presence of PCM emission even when the mode is red (blue) detuned from the QD resonances by as much as 20 nm (5 nm); (ii) Poissonian PCM emission; and (iii) antibunching in photon cross-correlation between PCM and excitonic luminescence. Remarkably, we did not observe any mode emission from PCMs fabricated in regions without QDs or when the QD was placed at the node of the PCM mode.

In Fig. 3, we show the key features of the aforementioned phenomenology for a deterministically coupled device where the first order PCM mode (M) was 19.4 nm red-detuned by a QD exciton (X). To carry out the photon cross-

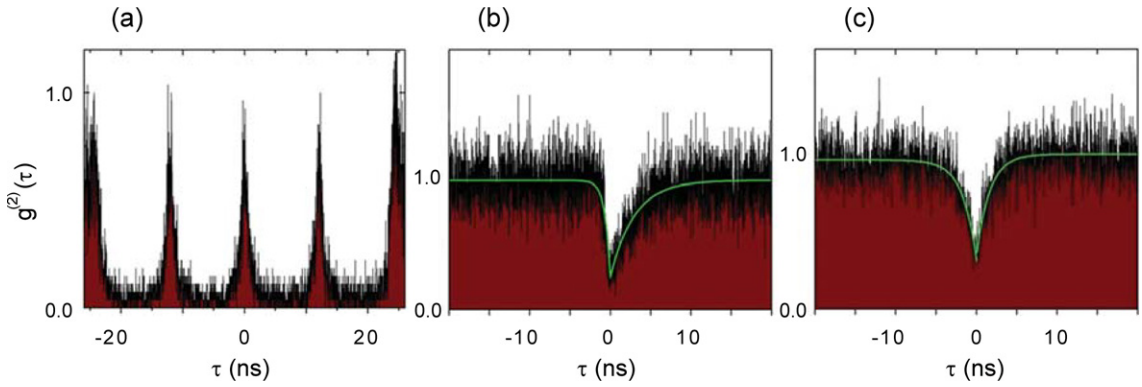

Fig. 3. (a) Normalized photon auto-correlation function of the PCM luminescence under pulsed excitation at the pump wavelength of 820 nm. (b), (c) Normalized second order cross-correlation functions ($g^{(2)}_{\mathrm{M,X}} = \langle : I_{\mathrm{M}}(t) I_{\mathrm{X}}(t+\tau) : \rangle / \langle : I_{\mathrm{M}}(t) \rangle \langle I_{\mathrm{X}}(t) \rangle$) between PCM and excitonic luminescence at pump wavelengths of (b) 780 nm and (c) 959 nm. In all cases the PCM mode (having $Q = 20\,000$) was red-detuned by 19.4 nm with respect to the lowest energy QD exciton transition.

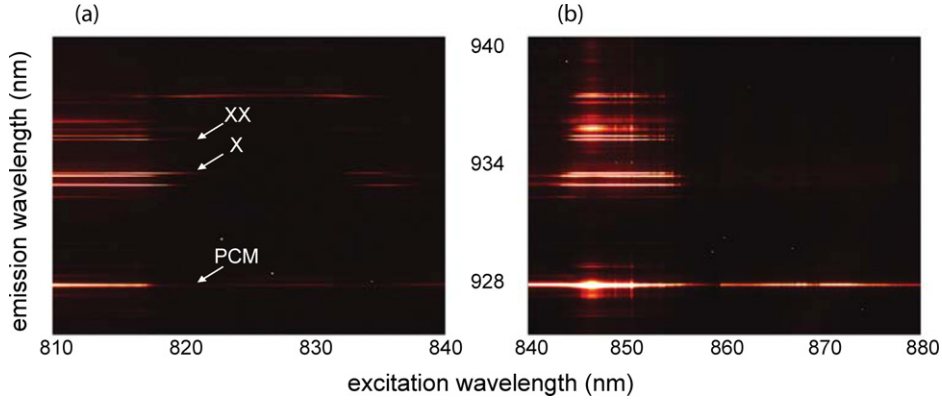

Fig. 4. Color plots of photoluminescence excitation (PLE) spectra when tuning the excitation wavelength. The excitation power was kept fixed with an electronic feedback. Neutral exciton (X) and biexciton (XX) emissions were identified by probing the fine structure as reported in Ref. [30]. (a) PLE in the pump wavelength range of 810–840 nm using a pump power of 50 nW. (b) PLE in the pump wavelength range of 840–880 nm using a pump power of 500 nW.

correlation ($g^{(2)}_{\mathrm{M,X}}$) measurements, we separated the two lines spectrally by the use of a diffraction grating and directed them individually to two avalanche photodiode (APD) single photon counting modules. The electrical pulses emitted upon photon detection were analyzed electronically using a time-to-amplitude converter followed by a multichannel analyzer that allowed for the accumulation of a histogram of coincidences with a given time delay.

Under pulsed excitation at the pump wavelength of 820 nm, we observed Poissonian PCM emission (Fig. 3(a)). Under continuous wave excitation, we show $g^{(2)}_{\mathrm{M,X}}$ at two different pump wavelengths 780 nm (Fig. 3(b)) and 959 nm (corresponding to the p-shell manifold of the QD) (Fig. 3(c)). For both pump wavelengths a clear anti-correlation can be observed, proving that emission of the PCM mode is quantum correlated with that of the QD. We observed the same antibunching behavior (at $\tau = 0$) for all the pump wavelengths we tested between GaAs band-gap and p-shell; the asymmetry in the cross-correlation signal that was dominant for short wavelength excitation disappeared for p-shell excitation.

To further characterize the different charging scenarios set by the excitation conditions, in Fig. 4 we show a color plot of the PL excitation (PLE) spectra when tuning the pumping wavelength (λ_{pump}) on a different device. Figs. 4(a) and 4(b) show data in the λ_{pump} range of 810–840 nm and 840–880 nm respectively. As the excitation laser crosses the GaAs band-edge, the total PL intensity decreases drastically both for the QD and the PCM mode. In the λ_{pump} region around 820–830 nm the exciton line around 937.5 nm dominates the spectrum while the PMC emission is reduced. This could be due to a prevalence of free electrons in the system, as excitation of the material occurs mainly via the

shallow acceptor states of the background carbon impurities [57]. Since for $\lambda_{pump} > 840$ nm the PL intensity reduces significantly, the spectra shown in Fig. 4(b) were taken at a pump power that is 10 times higher than those in Fig. 4(a). Here a clear resonance around 846 nm can be observed both for QD and PCM PL: the origin of this enhancement is unclear. As we approach the wetting layer band-edge (i.e. $\lambda_{pump} \approx 860$ nm) PL from the QD becomes negligible as compared to the PCM PL.

It is therefore clear that the qualitative behavior of the QD spectrum depends heavily on the excitation conditions. In particular there is only a limited excitation window in which the QD exhibits spectra that can be easily interpreted in terms of well-understood excitonic charge configurations. Usually this is the case for low pump powers in the vicinity of the GaAs band-edge and on the red side of the acceptor impurity levels (≈ 835 nm).

Acknowledgements

We would like to thank M. Atature, D. Gerace, and A. Reinhard for many helpful discussions. This work was supported by NCCR Quantum Photonics (NCCR QP), research instrument of the Swiss National Science Foundation (SNSF).

References

[1] S. Haroche, J.M. Raimond, Exploring the Quantum: Atoms, Cavities, and Photons, Oxford University Press, USA, 2006.
[2] J.M. Gerard, in: P. Michler (Ed.), Single Quantum Dots: Fundamentals, Application and New Concepts, in: Springer Series in Topics in Applied Physics, vol. 90, Springer, Berlin, 2003, p. 269.
[3] G. Khitrova, H.M. Gibbs, M. Kira, S.W. Koch, A. Scherer, Nature Phys. 2 (2006) 81–90.
[4] S. Noda, M. Fujita, T. Asano, Nature Photonics 1 (2007) 449–458.
[5] L. Jacak, P. Hawrylak, A. Wojs, Quantum Dots (NanoScience and Technology), Springer, 1998.
[6] D. Bimberg, M. Grundmann, N.N. Ledentsov, Quantum Dot Heterostructures, Wiley, 1999.
[7] P.M. Petroff, A. Lorke, A. Imamoglu, Physics Today 54 (2001) 46, and references therein.
[8] P. Michler, A. Kiraz, C. Becher, W.V. Schoenfeld, P.M. Petroff, L. Zhang, E. Hu, A. Imamoglu, Science 290 (2000) 2282.
[9] P. Borri, W. Langbein, S. Schneider, U. Woggon, R. Sellin, D. Ouyang, D. Bimberg, Phys. Rev. Lett. 87 (2001) 157401.
[10] C. Kammerer, C. Voisin, G. Cassabois, C. Delalande, Ph. Roussignol, F. Klopf, J.P. Reithmaier, A. Forchel, J.M. Gérard, Phys. Rev. B 66 (2002) R041306.
[11] M. Atature, J. Dreiser, A. Badolato, A. Hogele, K. Karrai, A. Imamoglu, Science 312 (2006) 551.
[12] K. Hennessy, A. Badolato, M. Winger, D. Gerace, M. Atature, S. Gulde, S. Faelt, E.L. Hu, A. Imamoglu, Nature 445 (2007) 896.
[13] T. Yoshie, A. Scherer, J. Hendrickson, G. Khitrova, H.M. Gibbs, G. Rupper, C. Ell, O.B. Shchekin, D.G. Deppe, Nature 432 (2004) 200.
[14] J.P. Reithmaier, G. Sek, A. Loffler, C. Hofmann, S. Kuhn, S. Reitzenstein, L.V. Keldysh, V.D. Kulakovskii, T.L. Reinecke, A. Forchel, Nature 432 (2004) 197.
[15] E. Peter, P. Senellart, D. Martrou, A. Lemaître, J. Hours, J.M. Gérard, J. Bloch, Phys. Rev. Lett. 95 (2005) 067401.
[16] D. Englund, A. Faraon, I. Fushman, N. Stoltz, P. Petroff, J. Vučković, Nature 450 (2007) 857–861.
[17] K. Srinivasan, O. Painter, Nature 450 (2007) 862–865.
[18] J.M. Lourtioz, H. Benisty, V. Berger, J.M. Gerard, Photonic Crystals: Towards Nanoscale Photonic Devices, Springer, 1999.
[19] Y. Takahashi, H. Hagino, Y. Tanaka, B.S. Song, T. Asano, S. Noda, Opt. Express 15 (2007) 17206–17213.
[20] S. Combrié, A. De Rossi, Q.V. Tran, H. Benisty, Appl. Phys. Lett. 90 (2007) 101118.
[21] A. Badolato, K. Hennessy, M. Atatüre, J. Dreiser, E. Hu, P.M. Petroff, A. Imamoglu, Science 308 (2005) 1158.
[22] J.M. Gérard, B. Sermage, B. Gayral, B. Legrand, E. Costard, V. Thierry-Mieg, Phys. Rev. Lett. 81 (1998) 1110.
[23] O.G. Schmidt, Lateral Alignment of Epitaxial Quantum Dots (Nanoscience and Technology), Springer, 2007.
[24] P. Gallo, M. Felici, B. Dwir, K.A. Atlasov, K.F. Karlsson, A. Rudra, A. Mohan, G. Biasiol, L. Sorba, E. Kapon, Appl. Phys. Lett. 92 (2008) 263101.
[25] T. Sünner, C. Schneider, M. Strauß, A. Huggenberger, D. Wiener, S. Höfling, M. Kamp, A. Forchel, Opt. Lett. 33 (2008) 1759.
[26] A. Dousse, L. Lanco, J. Suffczynski, E. Semenova, A. Miard, A. Lemaître, I. Sagnes, C. Roblin, J. Bloch, P. Senellart, arXiv: 0807.4427v1 [cond-mat.mtrl-sci].
[27] Y. Akahane, T. Asano, B.S. Song, S. Noda, Nature 425 (2003) 944.
[28] S. Strauf, K. Hennessy, M.T. Rakher, Y.-S. Choi, A. Badolato, L.C. Andreani, E.L. Hu, P.M. Petroff, D. Bouwmeester, Phys. Rev. Lett. 96 (2006) 127404.
[29] C.F. Wang, A. Badolato, I. Wilson-Rae, P.M. Petroff, E. Hu, J. Urayama, A. Imamoglu, Appl. Phys. Lett. 85 (2004) 3423.
[30] M. Winger, A. Badolato, K. Hennessy, E.L. Hu, A. Imamoglu, arXiv: 0808.2890v1 [cond-mat.mes-hall], Phys. Rev. Lett., in press.
[31] K. Hennessy, C. Reese, A. Badolato, C.F. Wang, A. Imamoglu, P.M. Petroff, E. Hu, G. Jin, S. Shi, D.W. Prather, Appl. Phys. Lett. 83 (2003) 3650.
[32] K. Srinivasan, O. Painter, Appl. Phys. Lett. 90 (2007) 031114.
[33] A. Rastelli, A. Ulhaq, S. Kiravittaya, L. Wang, A. Zrenner, O.G. Schmidt, Appl. Phys. Lett. 90 (2007) 073120.
[34] M. Pelton, C. Santori, J. Vučković, B. Zhang, G.S. Solomon, J. Plant, Y. Yamamoto, Phys. Rev. Lett. 89 (2002) 233602.

[35] N.G. Stoltz, M. Rakher, S. Strauf, A. Badolato, D.D. Lofgreen, P.M. Petroff, L.A. Coldren, D. Bouwmeester, Appl. Phys. Lett. 87 (2005) 031105.
[36] S. Strauf, N.G. Stoltz, M.T. Rakher, L.A. Coldren, P.M. Petroff, D. Bouwmeester, Nature Photonics 1 (2007) 704.
[37] H. Lohmeyer, J. Kalden, K. Sebald, C. Kruse, D. Hommel, J. Gutowski, Appl. Phys. Lett. 92 (2008) 011116.
[38] K. Hennessy, A. Badolato, A. Tamboli, P.M. Petroff, E. Hu, M. Atatüre, J. Dreiser, A. Imamoglu, Appl. Phys. Lett. 87 (2005) 021108.
[39] K. Hennessy, C. Högerle, E. Hu, A. Badolato, A. Imamoglu, Appl. Phys. Lett. 89 (2006) 041118.
[40] A.F. Koenderink, M. Kafesaki, B.C. Buchler, V. Sandoghdar, Phys. Rev. Lett. 95 (2005) 153904.
[41] F. Intonti, S. Vignolini, F. Riboli, A. Vinattieri, D.S. Wiersma, M. Colocci, L. Balet, C. Monat, C. Zinoni, L.H. Li, R. Houdré, M. Francardi, A. Gerardino, A. Fiore, M. Gurioli, Phys. Rev. B 78 (2008) 041401(R).
[42] S. Mujumdar, A.F. Koenderink, T. Sünner, B.C. Buchler, M. Kamp, A. Forchel, V. Sandoghdar, Opt. Express 15 (2007) 17214.
[43] S. Mosor, J. Hendrickson, B.C. Richards, J. Sweet, G. Khitrova, H.M. Gibbs, T. Yoshie, A. Scherer, Appl. Phys. Lett. 87 (2006) 141105.
[44] S. Strauf, M.T. Rakher, I. Carmeli, K. Hennessy, C. Meier, A. Badolato, M.J.A. DeDood, P.M. Petroff, E.L. Hu, E.G. Gwinn, D. Bouwmeester, Appl. Phys. Lett. 88 (2006) 043116.
[45] C.P. Michael, K. Srinivasan, T.J. Johnson, O. Painter, K.H. Lee, K. Hennessy, H. Kim, E. Hu, Appl. Phys. Lett. 90 (2007) 051108.
[46] L.C. Andreani, G. Panzarini, J.M. Gerard, Phys. Rev. B 60 (1999) 13276–13279.
[47] Y. Yamamoto, A. Imamoglu, Mesoscopic Quantum Optics, Wiley, 1999.
[48] S. Pau, G. Bjork, J. Jacobson, H. Cao, Y. Yamamoto, Phys. Rev. B 51 (1995) 14437–14447.
[49] G. Rempe, H. Walther, N. Klein, Phys. Rev. Lett. 58 (1987) 353–356.
[50] M. Brune, F. Schmidt-Kaler, A. Maali, J. Dreyer, E. Hagley, J.M. Raimond, S. Haroche, Phys. Rev. Lett. 76 (1996) 1800–1803.
[51] D.I. Schuster, A.A. Houck, J.A. Schreier, A. Wallraff, J.M. Gambetta, A. Blais, L. Frunzio, J. Majer, B. Johnson, M.H. Devoret, S.M. Girvin, R.J. Schoelkopf, Nature 445 (2007) 515–518.
[52] I. Schuster, A. Kubanek, A. Fuhrmanek, T. Puppe, P.W.H. Pinkse, K. Murr, G. Rempe, Nature Phys. 4 (2008) 382–385.
[53] K.M. Birnbaum, A. Boca, R. Miller, A.D. Boozer, T.E. Northup, H.J. Kimble, Nature 436 (2005) 87–90.
[54] M. Kaniber, A. Laucht, A. Neumann, J.M. Villas-Bôas, M. Bichler, M.-C. Amann, J.J. Finley, Phys. Rev. B 77 (2008) 161303(R).
[55] D. Press, S. Gotzinger, S. Reitzenstein, C. Hofmann, A. Loffler, M. Kamp, A. Forchel, Y. Yamamoto, Phys. Rev. Lett. 98 (2007) 117402.
[56] A. Badolato, M. Winger, K. Hennessy, E.L. Hu, A. Imamoglu, in preparation.
[57] W.-H. Chang, H.-S. Chang, W.-Y. Chen, T.M. Hsu, T.-P. Hsieh, J.-I. Chyi, N.-T. Yeh, Phys. Rev. B 72 (2005) 233302.